

UHI Research Database pdf download summary

Plankton community respiration and bacterial metabolism in a North Atlantic Shelf Sea during spring bloom development (April 2015)

Garcia-Martin, E Elena; Daniels, Chris; Davidson, Keith; Lozano, Jose; Mayers, Kyle; Mcneill, Sharon; Mitchell, Elaine; Poulton, Alex; Purdie, Duncan; Tarran, Glen; Whyte, Callum; Robinson, Carol

Published in:
Progress in Oceanography

Publication date:
2019

The re-use license for this item is:
CC BY-ND

The final published version is available direct from the publisher website at:
[10.1016/j.pocean.2017.11.002](https://doi.org/10.1016/j.pocean.2017.11.002)

[Link to author version on UHI Research Database](#)

Citation for published version (APA):

Garcia-Martin, E. E., Daniels, C., Davidson, K., Lozano, J., Mayers, K., Mcneill, S., Mitchell, E., Poulton, A., Purdie, D., Tarran, G., Whyte, C., & Robinson, C. (2019). Plankton community respiration and bacterial metabolism in a North Atlantic Shelf Sea during spring bloom development (April 2015). *Progress in Oceanography*, 177, Article 101873. <https://doi.org/10.1016/j.pocean.2017.11.002>

General rights

Copyright and moral rights for the publications made accessible in the UHI Research Database are retained by the authors and/or other copyright owners and it is a condition of accessing publications that users recognise and abide by the legal requirements associated with these rights:

- 1) Users may download and print one copy of any publication from the UHI Research Database for the purpose of private study or research.
- 2) You may not further distribute the material or use it for any profit-making activity or commercial gain
- 3) You may freely distribute the URL identifying the publication in the UHI Research Database

Take down policy

If you believe that this document breaches copyright please contact us at RO@uhi.ac.uk providing details; we will remove access to the work immediately and investigate your claim.

Plankton community respiration and bacterial metabolism in a North Atlantic Shelf Sea during spring bloom development (April 2015)

E. Elena García-Martín^{1*}, Chris J. Daniels², Keith Davidson³, Jose Lozano⁴, Kyle M. J. Mayers^{2,5}, Sharon McNeill³, Elaine Mitchell³, Alex J. Poulton^{2,6}, Duncan A. Purdie⁵, Glen A. Tarran⁷, Callum Whyte³, Carol Robinson¹

¹ Centre for Ocean and Atmospheric Sciences, School of Environmental Sciences, University of East Anglia, Norwich Research Park, Norwich, NR4 7TJ, UK.

² Ocean Biogeochemistry and Ecosystems, National Oceanography Centre, Waterfront Campus, European Way, Southampton SO14 3ZH, UK

³ Scottish Association for Marine Science, Scottish Marine Institute, Oban, Argyll, PA371QA, Scotland, UK

⁴ Departamento Ecología y Biología animal / ECIMAT, Facultad de Ciencias del Mar, Universidad de Vigo, CP 36210 Vigo, Spain.

⁵ Ocean and Earth Science, University of Southampton, National Oceanography Centre Southampton, Southampton, SO14 3ZH, UK

⁶ The Lyell Centre, Heriot-Watt University, Edinburgh, UK

⁷ Plymouth Marine Laboratory, Prospect Place, Plymouth, PL1 3DH, UK

* Corresponding author: Centre for Ocean and Atmospheric Sciences, School of Environmental Sciences, University of East Anglia, Norwich Research Park, Norwich, NR4 7TJ, UK.

Email address: Enma.Garcia-Martin@uea.ac.uk. Tel: 0044 (0)1603 593162

1 ABSTRACT

2 Spring phytoplankton blooms are important events in Shelf Sea pelagic systems as the
3 increase in carbon production results in increased food availability for higher trophic levels
4 and the export of carbon to deeper waters and the sea-floor. It is usually accepted that the
5 increase in phytoplankton abundance and production is followed by an increase in plankton
6 respiration. However, this expectation is derived from field studies with a low temporal
7 sampling resolution (5 - 15 days). In this study we have measured the time course of plankton
8 abundance, gross primary production, plankton community respiration, respiration of the
9 plankton size classes ($>0.8 \mu\text{m}$ and $0.2\text{-}0.8 \mu\text{m}$) and bacterial production at ≤ 5 day intervals
10 during April 2015 in order to examine the phasing of plankton autotrophic and heterotrophic
11 processes. Euphotic depth-integrated plankton community respiration increased five-fold
12 (from $22 \pm 4 \text{ mmol O}_2 \text{ m}^{-2} \text{ d}^{-1}$ on 4th April to $119 \pm 4 \text{ mmol O}_2 \text{ m}^{-2} \text{ d}^{-1}$ on 15th April) at the
13 same time as gross primary production also increased five-fold, (from 114 ± 5 to 613 ± 28
14 $\text{mmol C m}^{-2} \text{ d}^{-1}$). Bacterial production began to increase during the development of the
15 bloom, but did not reach its maximum until 5 days after the peak in primary production and
16 plankton respiration. The increase in plankton community respiration was driven by an
17 increase in the respiration attributable to the $>0.8 \mu\text{m}$ size fraction of the plankton community
18 (which would include phytoplankton, microzooplankton and particle attached bacteria).
19 Euphotic depth-integrated respiration of the $0.2\text{-}0.8 \mu\text{m}$ size fraction (predominantly free
20 living bacteria) decreased and then remained relatively constant (16 ± 3 - $11 \pm 1 \text{ mmol O}_2 \text{ m}^{-2}$
21 d^{-1}) between the first day of sampling (4th April) and the days following the peak in
22 chlorophyll-*a* (20th and 25th April). Recent locally synthesized organic carbon was more than
23 sufficient to fulfil the bacterial carbon requirement in the euphotic zone during this
24 productive period. Changes in bacterial growth efficiencies (BGE, the ratio of bacterial
25 production to bacterial carbon demand) were driven by changes in bacterial production rates

26 increasing from $<30 \pm 14$ % on 4th April to 51 ± 11 % on 25th of April. This study therefore
27 shows a concurrent rather than a phased increase in primary production and community
28 respiration attributable to cells $> 0.8 \mu\text{m}$ during the development of the spring bloom,
29 followed 5 days later by a peak in bacterial production. In addition, the size fractionated
30 respiration rates and high growth efficiencies suggest that free living bacteria are not the
31 major producers of CO_2 before, during and a few days after this shelf sea spring
32 phytoplankton bloom.

33 **Keywords:** plankton community respiration, bacterial metabolism, bacterial growth
34 efficiencies, Celtic Sea, spring bloom.

35 *1. Introduction*

36 Reduced water column turbulence is one of the principal factors governing the rapid increase
37 in plankton abundance in western-European shelf seas, such as the Celtic Sea, during spring
38 (Pingree et al. 1976; Fasham et al. 1983; Taylor et al. 1997; Smyth et al. 2014). The increase
39 in water column stability, the presence of high nutrient concentrations and ample light in the
40 surface mixing layer trigger an increase in primary production, and therefore an increase in
41 phytoplankton abundance (Joint et al. 2001; Behrenfeld 2010). Most of the studies of
42 temperate spring “blooms” of phytoplankton focus on the rapid increase in primary
43 production and the succession of phytoplankton groups (Joint et al. 1986; Widdicombe et al.
44 2010; Fileman et al. 2011; Barnes et al. 2015; Daniels et al. 2015). Only two studies have
45 measured both plankton production and plankton respiration during a spring bloom with the
46 temporal resolution (≤ 1 week) required to discern the short term phasing between primary
47 production and respiration (Blight et al. 1995; Caffrey et al. 1998). These studies in coastal
48 waters of the UK (Blight et al. 1995) and the USA (Caffrey et al. 1998) showed a time lag of
49 5-15 days between the maximum rate of primary production and the maximum rate of

50 community respiration. Blight et al. (1995) explained the delay in the respiration response to
51 be due to the time required for phytoplankton derived dissolved organic matter (DOM) to
52 become available to the bacteria.

53 DOM exuded by phytoplankton or made available by zooplankton sloppy feeding is
54 composed of high- and low-molecular weight compounds (Lancelot 1984; Biddanda and
55 Benner 1997). High molecular weight compounds are easily and rapidly assimilated by
56 bacteria (Amon and Benner 1994). Therefore, production of high molecular weight
57 compounds could stimulate an increase in heterotrophic bacterial respiration and production
58 on short time scales of hours to days as observed in microcosm addition experiments (Amon
59 and Benner 1994, Amon and Benner 1996, Lønborg et al. 2016). This concurrent increase in
60 primary production and bacterial production has also been observed in a spring bloom study
61 which sampled at daily intervals (Ducklow et al. 1993). However, due to logistics, the
62 sampling frequency in natural field studies is usually greater than this (i.e. weeks rather than
63 hours - days) and this longer sampling interval could miss the concurrent increase in
64 phytoplankton production and bacterial activity.

65 The activity of the microbial foodweb alters the biochemical composition of the
66 phytoplankton derived dissolved and particulate organic matter (Fernández et al. 1992;
67 Grossart et al. 2006; Danger et al. 2007), which then influences bacterial growth efficiencies
68 (BGE, the ratio of bacterial production to bacterial carbon demand) and in the long term, the
69 balance between production of CO₂, transfer of carbon to higher trophic groups and export
70 and storage of carbon in deeper waters. Despite the importance of understanding the temporal
71 variability in bacterial growth efficiency to quantification of the cycling of carbon, there have
72 been no previous measurements of BGE on temporal scales <1 week during spring bloom
73 events.

74 The aim of this study is to explain the temporal evolution of plankton community respiration
75 and bacterial metabolism (production, respiration and the bacterial growth efficiency) during
76 a spring bloom event at a shelf sea station and to determine the phasing between these
77 processes and primary production at short temporal scales (≤ 5 days). A companion paper in
78 this special issue incorporates these spring time data into a broader synthesis of the annual
79 and spatial variability in plankton dynamics of the Celtic Sea (García-Martín et al. this issue).

80

81 *2. Material and methods*

82 **2.1 Study site and sampling procedure**

83 A four week study was conducted during April 2015 at a single station in the centre of the
84 Celtic Sea (Central Celtic Sea, CCS, 49.39 °N, 8.58 °W, Fig. 1) where the water depth was
85 approximately 147 m. Depth profiles of temperature and salinity were measured using a
86 conductivity-temperature-depth (CTD) profiler (Sea-Bird Electronics, Washington, USA).
87 Water samples were collected pre-dawn (~03:00 GMT) from 7 depths on each of 6 occasions
88 (4th, 6th, 11th, 15th, 20th, 25th April) with 20-L Niskin bottles mounted on a rosette sampling
89 frame to which the CTD was attached. Six of these sample depths were in the euphotic zone,
90 considered as the depth at which incident irradiance is 1% of surface irradiance, (60, 40, 20,
91 10, 5 and 1 % of surface irradiance; Poulton et al. this issue), and one sample depth was
92 below the euphotic zone at 70 m. Seawater was carefully transferred from each of the Niskin
93 bottles into 10 L carboys for subsequent determination of plankton community respiration
94 derived from both dissolved oxygen consumption and the reduction of 2-(ρ -iodophenyl)-3-(ρ -
95 nitrophenyl)-5phenyl tetrazolium chloride (INT). The INT reduction method does not directly
96 measure respiration (Maldonado et al. 2012), but is a good proxy to estimate plankton and
97 bacterial respiration over short time scales (Martínez-García et al. 2009, Aranguren-Gassis et

98 al. 2012, García-Martín et al. 2016). Water samples for the determination of chlorophyll-*a*
99 (Chl-*a*), gross primary production (PP), heterotrophic bacterial production (BP) and bacterial
100 abundance (BA) were taken from the same Niskin bottles as the samples collected for the
101 determination of plankton community respiration. Sampling procedures followed Poulton et
102 al. (2016) for Chl-*a* (see also Hickman et al. this issue) and primary production (see also
103 Poulton et al. this issue), and Tarran et al. (2006) for bacterial abundance (see also Tarran et
104 al. this issue).

105 **2.2 Nutrients, total chlorophyll *a*, primary production and dissolved organic carbon** 106 **production**

107 Nitrate+nitrite and phosphate concentrations were analysed on board using a Bran and
108 Luebbe segmented flow colorimetric auto-analyser using classical analytical techniques as
109 described in Woodward and Rees (2001). Water samples were collected directly from the
110 Niskin bottles at each station. Clean sampling and handling techniques were employed, and
111 where possible were carried out according to the International GO-SHIP recommendations
112 (Hydes et al. 2010). Nutrient reference materials (KANSO Japan) were run each day to check
113 analyser performance and to guarantee the quality of the final reported data. The typical
114 uncertainty of the analytical results was between 2 – 3 %, and the limits of detection were
115 0.02 $\mu\text{moles L}^{-1}$ for nitrate+nitrite and phosphate. All samples were analysed within 1-2 hours
116 of sampling. Nutrient data are presented in Humphreys et al. (this issue).

117

118 Samples for total Chl-*a* were collected by filtering 200-250 mL of sea water through 25 mm
119 diameter Fisherbrand MF300 or Whatman GF/F filters (effective pore size 0.7 μm). After
120 filtration, pigments were extracted in 90 % acetone for 18 to 20 h in the dark at 4 °C.
121 Chlorophyll *a* concentration was determined fluorometrically on a Turner Trilogy

122 fluorometer using a non-acidification module and calibrated with a pure chlorophyll-*a*
123 standard (Sigma-301 Aldrich, UK). Instrument drift was monitored and adjusted for using a
124 solid-secondary standard (Turner Designs).

125 Daily rates of particulate gross primary production were scaled up from short-term (6-8 h,
126 dawn to midday) rates of carbon fixation to seasonally adjusted day lengths (14 h in April).
127 Rates of dissolved organic carbon production (*p*DOC) were determined at three depths (60 %,
128 20 % and 1 % of surface irradiance) from the same bottles and incubations as for carbon
129 fixation using methods adapted from López-Sandoval et al. (2011) and Poulton et al. (2016).
130 It is expected that the daily rates of primary production presented in this paper based on
131 short-term (<8 h) incubations, better approximate 'gross primary production', whilst daily
132 rates presented in companion papers (Mayers et al. this issue; Poulton et al. this issue), based
133 on long-term (24 h) incubations better approximate 'net primary production' (see e.g. Marra
134 2002).

135 For carbon fixation and *p*DOC, water samples were collected into four 70 mL polycarbonate
136 bottles (3 light, 1 dark), and spiked with 6-11 μCi carbon14 (^{14}C) labelled sodium
137 bicarbonate. The bottles were then incubated in a purpose-built constant temperature
138 containerised laboratory at a range of seasonally adjusted irradiance levels (daily photon
139 fluxes) using LED light panels and neutral density filters. Day-light LED light panels
140 (Powerpax, UK) provided $100 \mu\text{mol photons m}^{-2} \text{ s}^{-1}$. Daily light doses were: 22.2, 13.1, 6.0,
141 3.4, 1.1 and $0.4 \text{ mol quanta m}^{-2} \text{ d}^{-1}$ (corresponding to 60, 40, 20, 10, 5 and 1% of surface
142 irradiance). The average surface irradiance for the cruise was $33.9 \text{ mol quanta m}^{-2} \text{ d}^{-1}$, range
143 $18.1 - 45.4 \text{ mol quanta m}^{-2} \text{ d}^{-1}$ (see Poulton et al. this issue). The incubation temperatures
144 were within $\pm 1 \text{ }^\circ\text{C}$ of the in situ temperature. On termination of the incubation, 5 mL sub-
145 samples were filtered through 25 mm $0.2 \mu\text{m}$ polycarbonate filters, with the filtrates
146 transferred to 20 mL scintillation vials for *p*DOC estimates. To remove the dissolved

147 inorganic ^{14}C , 100 μL of 50 % HCl was added to each vial, which were then sealed with a
148 gas-tight rubber septum (Kimble-Kontes) and a centre well (Kimble-Kontes) containing a
149 CO_2 trap (Whatman GFA filter soaked with 200 μL β -phenylethylamine) (see Mayers et al.
150 this issue). After 12 hours, the CO_2 traps were removed and disposed of, and 15 mL of
151 Ultima Gold (Perkin Elmer, UK) liquid scintillation cocktail was added to the filtrate. Spike
152 activity was checked following Mayers et al. (this issue) and activity in the filtrates was
153 determined in a Tri-Carb 3100TR Liquid Scintillation Counter.

154 The remainder of each sample was then filtered through 25 mm 0.4 μm polycarbonate filters
155 (NucleporeTM, USA), with extensive rinsing to remove any unfixed ^{14}C -labelled sodium
156 bicarbonate, and 12 mL of Ultima Gold (Perkin-Elmer, UK) liquid scintillation cocktail
157 added. The activity on the filters was then determined using a Tri-Carb 3100TR Liquid
158 Scintillation Counter on-board. The average coefficient of variation was 9 % (range <1 to 74
159 %, with higher coefficients of variation associated with low rates at the base of the euphotic
160 zone).

161 **2.3 Bacterial abundance**

162 Samples for the enumeration of bacteria were collected from the Niskin bottles into clean 250
163 mL polycarbonate bottles. Subsamples were then pipetted into 2 mL microcentrifuge tubes
164 and fixed with glutaraldehyde (50%, TEM grade, 0.5% final concentration) within 30
165 minutes of collection. After fixing for 30 min at 4 °C, samples were stained with SYBR
166 Green I DNA dye (Invitrogen) for 1 h at room temperature in the dark and then analysed by
167 flow cytometry (Tarran et al. 2006). The mean coefficient of variation for the flow cytometric
168 analysis of bacterial abundance (BA) following this protocol was 2.3 %, based on the means
169 and standard deviations of 160 sets of duplicate and triplicate bacterial abundance analyses
170 from Station L4 of the Western English Channel Observatory, Plymouth, UK.

171 **2.4 Respiration derived from dissolved oxygen consumption**

172 Five of the 6 light depths detailed above (60, 40 or 20, 10, 5 and 1 % of surface irradiance)
173 and the sample depth below the euphotic zone, were sampled for plankton community
174 respiration (CR_{O_2}). CR_{O_2} was determined by measuring the decrease in dissolved oxygen
175 after a 24 h incubation in the dark. Dissolved oxygen concentration was measured by
176 automated Winkler titration performed with a Metrohm 765 burette to a photometric end
177 point (Carritt and Carpenter 1966). Ten gravimetrically calibrated 60 mL borosilicate glass
178 bottles were carefully filled with seawater from each 10 L carboy. Water was allowed to
179 overflow during the filling, and care was taken to prevent air bubble formation in the silicone
180 tube. Five bottles were fixed at the start of the incubation (“zero”) with 0.5 mL of 3 M
181 manganese sulphate and 0.5mL of 4 M sodium iodide/8 M sodium hydroxide solution (Carritt
182 and Carpenter 1966). The remaining five bottles were placed underwater in darkened
183 temperature controlled incubators located in a temperature controlled room for 24 h (“dark”).
184 The incubation temperatures were within ± 0.5 °C of the in situ temperature. “Dark” bottles
185 were fixed as described for the “zero” bottles after 24 h. Daily plankton community
186 respiration was calculated from the difference in oxygen concentration between the mean of
187 the replicate “zero” measurements and the mean of the replicate “dark” measurements,
188 assuming a linear decrease over 24h. The standard error (\pm SE) of the net change was
189 calculated as the square root of the sum of the squares of the SEs of the “zero” and “dark”
190 replicates.
191 The average percentage coefficient of variation was 0.15% for both the “zero” and “dark”
192 replicate oxygen concentrations ($n = 36$ in each case).

193 **2.5 Respiration derived from INT reduction**

194 Five 200 mL dark glass bottles were filled with seawater from each 10 L carboy. Two
195 replicates were immediately fixed by adding formaldehyde (2% w/v final concentration) and
196 used as controls. All five bottles were then inoculated with a sterile solution of 7.9 mM 2-(p-
197 iodophenyl)-3-(p-nitrophenyl)-5phenyl tetrazolium chloride (INT) to give a final
198 concentration of 0.8 mM. The solution was freshly prepared for each experiment using Milli-
199 Q water. Samples (+ controls) were incubated in the same temperature-controlled water bath
200 as the dissolved oxygen bottles for 0.5 to 0.8 h. Incubations were terminated by adding
201 formaldehyde to the three replicates, as done previously for the controls. Each sample and
202 control were then filtered through 0.8 μm and onto 0.2 μm pore size polycarbonate filters,
203 and the filters were air-dried, and stored frozen. The INT reduced in each size fraction (i.e.
204 $>0.8 \mu\text{m}$ and $0.2\text{-}0.8 \mu\text{m}$) was extracted with propanol and the absorbance at 485 nm
205 determined using a Beckman model DU640 spectrophotometer following Martínez-García et
206 al. (2009). The INT reduced was calculated as the average INT reduced in the three incubated
207 samples minus the average of the INT reduced in the two controls for each size fraction.
208 Thus, the measurements are corrected for any interference by the absorbance of the water due
209 to turbidity or reduction of INT caused by non-metabolic factors (i.e. organic matter content).
210 The rate measured in the large size-fraction ($\text{INT}_{>0.8}$) will result mainly from INT reduction
211 by eukaryotes and particle-attached bacteria. Since the combined abundance of
212 *Synechococcus* and *Prochlorococcus* made up only 1% of the total abundance of
213 *Synechococcus*, *Prochlorococcus* and bacteria (data not shown), the main respiring organisms
214 in the small size-fraction ($\text{INT}_{0.2\text{-}0.8}$) are expected to be free living heterotrophic bacteria. The
215 total plankton community respiration (INT_T) in $\mu\text{mol INT}_f \text{ L}^{-1} \text{ h}^{-1}$ is calculated as the sum of
216 the INT reduction in the two size fractions ($\text{INT}_{0.2\text{-}0.8}$ and $\text{INT}_{>0.8}$).

217 A time-course experiment was carried out on water collected from 5 m on the 4th of April
218 2015 in order to determine the optimal incubation time for INT reduction. The maximum

219 incubation time before the INT became toxic for the plankton community (and so the rate of
220 INT reduction began to decrease) was 1 h and hence all our incubations were undertaken for
221 0.5 to 0.8 h. The INT reduction technique, which includes a post-incubation filtration and an
222 incubation <1 hour, allows the determination of more realistic rates of bacterial respiration
223 than the traditional 0.8 μm pre-filtered 24 hour bottle incubation technique (Aranguren-
224 Gassis et al. 2012). INT reduction was converted into units of oxygen consumption by
225 applying the equation $\text{Log O}_2 = 0.80\text{Log INT}_T + 0.45$ ($R^2 = 0.43$, $p < 0.0001$, $n = 97$) derived
226 from the comparison of the 97 concurrent measurements of CR_{O_2} and INT_T rates measured
227 during November 2014, April and July 2015 (see Garcia-Martin et al. this issue and
228 Supplementary Figure 1).

229 Plankton and bacterial respiration in units of O_2 consumption were then converted into units
230 of carbon production using a constant respiratory quotient of 1 (Buchanan et al. 2000,
231 Williams and del Giorgio 2005). We are aware that plankton and bacterial respiratory
232 quotients are not constant and vary according to the composition of the substrate being
233 oxidized (Berggren et al. 2012, Robinson and Williams 1999, Williams and del Giorgio
234 2005). However, without any information on substrate composition we have to assume a
235 constant value and accept an error associated with this conversion of ~20 %.

236 **2.6 Heterotrophic bacterial production and bacterial growth efficiency**

237 Bacterial production (BP) was calculated from ^{14}C leucine incorporation using a theoretical
238 approach assuming no isotope dilution (Kirchman 2001). Water samples (125 mL) were
239 collected from the same 6 Niskin bottles as those sampled for plankton respiration detailed
240 above, into acid-washed polycarbonate bottles. Aliquots of 10 μL ^{14}C leucine working
241 solution (0.04 MBq mL^{-1}) were pipetted into 2 mL sterile centrifuge tubes with 1.6 mL of
242 sample water and mixed.

243 For each depth two replicates were incubated for 0, 1, 2 and 3 h in the dark at in situ
244 temperatures. Samples were fixed with 80 μL of 20 % paraformaldehyde (final concentration
245 of 1 %) and filtered onto 0.2 μm polycarbonate filters (pre-soaked in 1 mM non-labelled
246 leucine). Sample vials were washed with deionised water to rinse any remaining label from
247 each vial. Then filters were inserted into scintillation vials, dried overnight at room
248 temperature and mixed with 4 mL of Optiphase Hi-Safe II scintillation fluid. Radioactivity in
249 the samples was measured using a Beckman Coulter LS6500 liquid scintillation counter with
250 the efficiency of counting determined using the external quench monitor method. [^{14}C]leucine
251 incorporation was calculated from counts (corrected for quenching) according to Kirchman
252 (2001) using isotope specific activity values corrected for decay (Stewart and Hawcroft,
253 1977). Bacterial production was derived from the slope of a regression of the disintegrations
254 per minute at the 4 incubation times. The precision of the technique ranged from 0.0003 to
255 0.0112 with a median value of 0.0027 $\mu\text{g C L}^{-1} \text{d}^{-1}$.

256 Cell-specific bacterial production and respiration were calculated by dividing BP and $\text{INT}_{0.2-}$
257 $_{0.8}$ by BA, respectively. Bacterial carbon demand (BCD) was calculated as: $\text{BCD} = \text{BP} +$
258 $\text{INT}_{0.2-0.8}$ and bacterial growth efficiency (BGE) as: BP/BCD .

259 **2.7 Data analysis**

260 Euphotic depth integrated CR_{O_2} , INT_{T} , $\text{INT}_{0.2-0.8}$, PP and BP rates were calculated by
261 trapezoidal integration of the volumetric rates measured at the five depths within the euphotic
262 depth. The standard errors ($\pm \text{SE}$) of the integrated rates were calculated following the
263 propagation procedure for independent measurements described by Miller and Miller (1988).
264 The depth-integrated contribution of the 0.2 to 0.8 μm fraction to total plankton community
265 respiration ($\% \text{INT}_{0.2-0.8}$) was calculated as the depth-integrated $\text{INT}_{0.2-0.8}$ divided by the
266 depth-integrated INT_{T} and multiplied by 100.

267 Statistical analyses were performed with SPSS software. Spearman non-parametric
268 correlation tests were used to study the relationship between volumetric CR_{O2}, INT_T, INT_{0.2-}
269 _{0.8}, PP and BP and between each of these and other physicochemical and biological
270 parameters (temperature, nitrate+nitrite and phosphate concentration, Chl-*a* concentration,
271 bacterial abundance).

272 Figure 2 was produced with Ocean Data View (ODV) software (Schlitzer 2015).

273

274 3. *Results*

275 3.1 Hydrographic and nutrient conditions

276 A full description of the hydrographic and nutrient conditions present at CCS between 4th
277 April and 25th April 2015 is presented in Wihsgott et al. (this issue) and Humphreys et al.
278 (this issue) and a brief overview is given in Table 1. The water column was stratified with a
279 pycnocline at 51 to 47 m at the beginning of the sampling period (4th and 6th April) (Fig. 2)
280 with colder and less saline waters at the surface. The depth of the euphotic zone decreased
281 after the 6th of April when the pycnocline also shoaled to less than 47 m (Table 1). Nutrient
282 concentrations were vertically homogenous in the water column during the first two sampling
283 days (4th and 6th April) with high concentrations of nitrate+nitrite and phosphate ($\sim 6 \pm 0.07$
284 $\mu\text{mol L}^{-1}$ and $\sim 0.5 \pm 0.01 \mu\text{mol L}^{-1}$, respectively) (Humphreys et al. this issue). Nutrient
285 concentrations decreased above the pycnocline over the following 15 days to a nitrate+nitrite
286 concentration of 0.4 to 0.7 $\mu\text{mol L}^{-1}$ and a phosphate concentration between 0.13 and 0.15
287 $\mu\text{mol L}^{-1}$ on the 25th April. Nutrients remained high below the pycnocline, in the aphotic
288 zone, and a marked nitracline developed at ~ 20 m.

289 3.2 Total chlorophyll-*a* and primary production

290 Chlorophyll-*a* vertical profiles showed a well-mixed distribution during 4th and 6th April (Fig.
291 3A). After this time, the vertical distribution of Chl-*a* was characterized by higher (sub-)
292 surface (5 -16 m) values and a progressive decrease with depth. Maximum values were
293 recorded on the 15th of April with surface values of 7.7 $\mu\text{g Chl-}a \text{ L}^{-1}$ and a maximum Chl-*a* of
294 8.4 $\mu\text{g Chl-}a \text{ L}^{-1}$ at 16 m. Chl-*a* concentrations decreased sharply between the 15th and 20th
295 April, and measured 3.7 $\mu\text{g Chl-}a \text{ L}^{-1}$ on the 25th April. Chl-*a* values at the base of the
296 euphotic layer were similar throughout the sampling period ($<2 \mu\text{g Chl-}a \text{ L}^{-1}$).

297 Primary production profiles showed a similar temporal pattern to Chl-*a* with low rates in
298 surface waters on the first two days ($<8 \mu\text{mol C L}^{-1} \text{ d}^{-1}$) increasing to 19.9 $\mu\text{mol C L}^{-1} \text{ d}^{-1}$
299 on the 11th April and reaching maximum values on the 15th April ($\sim 40 \mu\text{mol C L}^{-1} \text{ d}^{-1}$) (Fig.
300 3B). Primary production had decreased by the 20th April to similar values as on the 11th of
301 April and remained at these rates until the 25th April (Fig. 3B).

302 Euphotic zone depth-integrated gross primary production increased >5 -fold between the 4th
303 and the 15th of April, decreased by $\sim 50\%$ between the 15th and the 20th of April and then
304 remained relatively stable until the 25th of April (Table 2).

305 **3.3 Bacterial abundance**

306 Bacterial abundance followed a similar temporal trend to Chl-*a* with a homogenous vertical
307 distribution during the first two days ranging from 0.75 to 0.86 $10^6 \text{ cells mL}^{-1}$ (Fig. 3C). On
308 the 11th April, when the euphotic depth became shallower, bacterial abundance increased to
309 $>1.2 \cdot 10^6 \text{ cells mL}^{-1}$ (Fig. 3C). However, whereas the peak in Chl-*a* occurred on the 15th April,
310 the highest bacterial abundance occurred on the 20th April ($1.9 \cdot 10^6 \text{ cells mL}^{-1}$). Bacterial
311 abundance decreased again by the 25th April ($0.74 \cdot 10^6 \text{ cells mL}^{-1}$) to values similar to those at
312 the beginning of the sampling period ($0.79 \cdot 10^6 \text{ cells mL}^{-1}$). There was no distinct increase in
313 bacterial abundance in the aphotic zone, with values remaining around 0.7 to 0.9 10^6 cells

314 mL⁻¹ for the period from the 4th to 20th April, decreasing to 0.2 10⁶ cells mL⁻¹ on the 25th
315 April.

316 **3.4 Plankton and bacterial metabolism**

317 There was a significant correlation between oxygen consumption ($\mu\text{mol O}_2 \text{ L}^{-1} \text{ d}^{-1}$) and INT
318 reduction ($\mu\text{mol INT}_f \text{ L}^{-1} \text{ h}^{-1}$) measured during April 2015 ($r = 0.78$, $p < 0.0001$, $n = 32$,
319 supplementary Figure 1 and 2), confirming the validity of the INT_T technique as a proxy for
320 plankton respiration and endorsing the conversion of INT reduction into units of oxygen
321 consumption (Fig. 4A).

322 Plankton community respiration (CR_{O2}) at ~10 m increased from $<1.4 \pm 0.49 \mu\text{mol O}_2 \text{ L}^{-1} \text{ d}^{-1}$
323 before the strengthening of the pycnocline (4th and 6th April) to $8.05 \pm 0.58 \mu\text{mol O}_2 \text{ L}^{-1} \text{ d}^{-1}$ on
324 the day of highest Chl-*a* (15th April) (Fig. 4B). CR_{O2} decreased to $<4.00 \pm 0.25 \mu\text{mol O}_2 \text{ L}^{-1} \text{ d}^{-1}$
325 ¹ by the 20th April, and increased again by the 25th. CR_{O2} in the aphotic zone varied relatively
326 little between the sampling days ($0.35 \pm 0.14 - 1.22 \pm 0.55 \mu\text{mol O}_2 \text{ L}^{-1} \text{ d}^{-1}$). Changes in
327 plankton respiration were mainly driven by changes in the respiration of the $>0.8 \mu\text{m}$ size
328 fraction (Fig. 4C).

329 Euphotic depth-integrated rates of CR_{O2} increased 5.4-fold from the 4th of April to the 15th of
330 April (Table 2) when the respiration maximum occurred in sub-surface waters (10 - 20 m),
331 and then decreased on the 20th of April at the same time as a decrease in depth-integrated PP.
332 The maximum depth-integrated respiration rate was observed on the 25th of April due to the
333 high respiration rates measured below 20 m.

334 There was a significant relationship between PP and CR_{O2} for the first 5 days ($r = 0.9$, $p =$
335 0.037 , $n = 5$) of the study, but not for the duration of the study ($r = 0.71$, $p = 0.11$, $n = 6$),
336 indicating a co-evolution of the two variables during the pre-bloom and bloom period (4th -
337 20th April), but not in the late post-bloom (25th April) when the highest depth-integrated

338 plankton respiration rate was measured while PP had intermediate values (Table 2 and
339 Supplementary Figure 3). The euphotic zone was net autotrophic ($PP > CR_{O_2}$) during the
340 whole sampling period with maximum values of $PP - CR_{O_2}$ on the 15th April ($490 \text{ mmol C m}^{-2}$
341 d^{-1}) (Table 2).

342 Free-living bacterial respiration ($INT_{0.2-0.8}$) was less variable over time than plankton
343 community respiration, and did not vary significantly with depth (Fig. 4D). Euphotic depth-
344 integrated bacterial respiration was $16.0 \pm 2.9 \text{ mmol O}_2 \text{ m}^{-2} \text{ d}^{-1}$ on the 4th April, decreasing to
345 $8.2 \pm 1.5 \text{ mmol O}_2 \text{ m}^{-2} \text{ d}^{-1}$ on the 11th April, and remained fairly constant until the 25th April
346 (Table 2).

347 The proportion of plankton community respiration attributable to free-living bacteria
348 ($\%INT_{0.2-0.8}$) was $37 \pm 10 \%$ at the beginning of the sampling period (4th and 6th April)
349 decreasing to around $16 \pm 3 \%$ on 15th April (Table 2). The decrease in $\%INT_{0.2-0.8}$ was due to
350 an increase in $INT_{>0.8}$.

351 Bacterial production in the upper 20 m increased from $\sim 1 \mu\text{g C L}^{-1} \text{ d}^{-1}$ on the 4th and 6th April
352 to a maximum of $3-5 \mu\text{g C L}^{-1} \text{ d}^{-1}$ on the 20th April (Fig. 4E). There was no difference in the
353 rates of BP on the 15th and 20th of April in the upper 18 m but there was a 1.5- to 4-fold
354 increase in rates in waters deeper in the euphotic zone. Bacterial production in the aphotic
355 zone remained consistently low between 0.59 ± 0.01 and $0.68 \pm 0.20 \mu\text{g C L}^{-1} \text{ d}^{-1}$. In contrast
356 to bacterial respiration, euphotic depth-integrated bacterial production rates increased 2.3-
357 fold before the Chl-*a* maximum on 15th April, and 2.8-fold by the maximum in bacterial
358 abundance on the 20th April (Table 2) which was 5 days after the maxima in Chl-*a*, PP, CR_{O_2}
359 and INT_T . The low bacterial numbers measured on the 25th April (Fig. 3C) were associated
360 with high bacterial production, suggesting greater metabolic efficiency. Bacterial production

361 was significantly correlated to PP ($r = 0.51$, $p = 0.004$, $n = 30$), with PP able to explain 28 %
362 of the variability in BP.

363 Cell-specific bacterial metabolism showed different trends for bacterial respiration and
364 production. There was no significant difference between cell-specific bacterial respiration
365 between days ($p > 0.5$, t-test) (Fig. 5A). However, cell-specific bacterial production increased
366 gradually during the development of the phytoplankton bloom (from 1.4 fg C cell⁻¹ d⁻¹ to 5.7
367 fg C cell⁻¹ d⁻¹) with maximum cell-specific production rates on 25th April as a consequence of
368 the lower bacterial abundance (Fig. 5B).

369 In order to get an indication of whether the local primary production could support the
370 bacterial carbon demand, the depth-integrated organic matter production (particulate and
371 dissolved) minus the autotrophic losses (considered as the INT_{>0.8}) was compared with the
372 bacterial carbon demand (BCD). Depth-integrated BCD ranged between 2.4 and 6.5 % of the
373 depth integrated organic matter available (Fig. 6), indicating that the organic carbon produced
374 by phytoplankton was between 20 and 40 times greater than the carbon requirements of the
375 bacteria.

376 Bacterial growth efficiencies (BGE) were lowest (high bacterial respiration associated with
377 low bacterial production) at the beginning of the spring bloom (<31 %) and increased on the
378 11th April to 40 - 60 %, remaining at this level until the 25th April (Fig. 4F). In general, the
379 greater variability in bacterial production was reflected in the variability in BGEs (Fig. 7A-B)
380 which were always higher in the euphotic zone than in the aphotic zone (range 13 – 22 %).

381

382 4. *Discussion*

383 April 2015 in the central Celtic Sea was characterised by a reduction in vertical mixing and
384 the formation of a well-stratified upper layer, typical for the spring period in shelf seas

385 (Pingree et al. 1976; Fasham et al. 1983). The change in the water column structure allowed
386 the initiation of a spring bloom (Henson et al. 2006, Wihsgott et al. this issue), seen as a sharp
387 increase in Chl-*a* concentration, which lasted less than 15 days (Fig. 3A). This brief but
388 intense increase in Chl-*a* is typical of spring-blooms in these temperate waters (Joint et al.
389 2001; Fileman et al. 2011). In ten days, depth-integrated Chl-*a* concentrations increased 3-
390 fold in the euphotic zone associated with a 5-fold increase in both gross primary production
391 and plankton community respiration (Table 2). The range in magnitude of primary production
392 was greater than the range in respiration in the euphotic layer (Table 2) during the spring
393 bloom period. There was a clear temporal trend in the balance between gross primary
394 production and respiration ($PP - CR_{O_2}$) increasing from the pre-bloom period to a maximum
395 on 15th of April alongside the maximum in Chl-*a*. There was a decrease in the $PP - CR_{O_2}$
396 balance after the bloom but it always remained positive. The higher production compared to
397 respiration indicates a high concentration of particulate organic matter available for export to
398 deeper waters or transfer to higher trophic levels. In fact, the concentrations of particulate
399 organic carbon (POC) in the aphotic layers, below the pycnocline, significantly increased
400 from 3 $\mu\text{mol L}^{-1}$ on 15th April to 5 $\mu\text{mol L}^{-1}$ on 20th April (Davis et al. this issue) suggesting
401 that a proportion of the excess POC was exported from the surface layers to deeper waters.
402 Phytoplankton can quickly adjust the amount of cellular pigments, antennae and reception
403 points to increase the efficiency of photosynthesis (Falkowski and Owens 1980; Moore et al.
404 2006) when nutrients and light are available. The restructuring of the photosynthetic
405 apparatus and the synthesis of new reaction centres are associated with a higher energetic
406 demand (Falkowski and Raven 1997), and presumably a higher rate of phytoplankton
407 respiration. This is consistent with our results and the fact that plankton community
408 respiration rates, and in particular the respiration associated with the size class $>0.8 \mu\text{m}$,
409 increased in parallel with the increases in the abundance of autotrophic dinoflagellates and

410 ciliates (Tarran et al. this issue) and gross primary production (Table 2) during the spring
411 bloom (see also Mayers et al. this issue; Poulton et al. this issue). Previous studies of spring
412 phytoplankton blooms based on a sampling interval of ca. 5-15 days also observed an
413 increase in plankton community respiration rates associated with an increase in production
414 (Blight et al. 1995; Caffrey et al. 1998) but with a time lag of ≤ 1 week (Caffrey et al. 1998) to
415 a fortnight (Blight et al. 1995). The higher sampling frequency in our study (2 – 5 days) than
416 in the former studies allowed us to observe the parallel increase in PP and CR_{O2}. This parallel
417 evolution would have been missed if our sampling frequency were reduced. For example if
418 we only consider data from the 4th, 15th and 25th of April, we would have inferred a
419 continuous increase in CR_{O2} with a maximum 10 days after the maximum in PP. However,
420 when our data from 6th, 11th and 20th are included, the concurrent patterns of increase and
421 decrease in both CR_{O2} and PP are revealed.

422 The occurrence or lack of a time lag between PP and CR_{O2} may be related to the plankton
423 community structure and the capacity of the plankton to react rapidly to an increase in
424 resources. In our study, nanophytoplankton (2 - 20 μm) dominated the bloom, both in terms
425 of cell abundance (Tarran et al. this issue), Chl-*a* and primary production (Hickman et al. this
426 issue), rather than the larger diatom and dinoflagellate taxa often considered to be typical of
427 spring blooms in this area (Rees et al. 1999; Widdicombe et al. 2010; Van Oostende et al.
428 2012). Plankton communities dominated by small and fast growing cells are characterised by
429 greater interactions between species and faster organic matter and energy cycling (Legendre
430 and Le Fèvre 1995; D'alelio et al. 2016) which could also contribute to the lack of a time lag
431 between the increase in production and respiration.

432 Blight et al. (1995) suggested that the time lag they observed was due to the organic matter
433 produced during a spring bloom only stimulating bacterial respiration a few days later.
434 However, this is not consistent with our results, where bacterial abundance and production

435 increased at the same time as the increase in Chl-*a*, reaching maxima on 20th April, 5 days
436 after the maxima of Chl-*a*, primary production and respiration of the plankton fraction >0.8
437 μm ($\text{INT}_{>0.8}$). The earlier maxima in primary production and plankton respiration compared to
438 bacterial abundance could be related to a grazing effect. Nanophytoplankton are known to be
439 active grazers on bacteria (Sherr and Sherr 1994) and could have controlled the bacterial
440 abundance during the pre-bloom period. Then, the increase of organic matter (particulate and
441 dissolved, data not shown) on the 15th April and the decrease in the >0.8 μm plankton
442 biomass (in terms of Chl-*a* and abundance, data not shown) observed on the 20th April may
443 have released the grazing pressure and stimulated a change in the bacterial community
444 composition (Smith et al. 1995; Azam 1998; Tada et al. 2011; Landa et al. 2015). In fact,
445 there was a 1.6-fold increase in the abundance of bacterial cells with high nucleic acid
446 content on the 15th of April and a 2.8-fold increase on the 20th of April compared to their
447 abundance on the 11th of April (Fig. 2, and see Tarran et al. this issue). As different bacteria
448 have different metabolic efficiencies, the phylotypes forming the bacterial community at the
449 end of April may have been rapidly growing bacteria with higher production rates (Pedler et
450 al. 2014). In addition, bacterial respiration was highest at the beginning of the sampling
451 period and then remained relatively constant during and up to 10 days after the Chl-*a*
452 maximum. This relative stability in bacterial respiration might be caused by a bias in the
453 sampling methodology as the respiration of particle attached bacteria is not included.
454 However, this problem is inherent to all studies where bacterial respiration is measured as the
455 respiration of a size-class of the plankton (e.g. Blight et al. 1995), and so it is unlikely to
456 explain the differences between our study and previous ones (Blight et al. 1995).

457 Depth-integrated BCD only accounted for < 6.5 % of the net organic matter locally produced
458 (production minus the autotrophic respiration), and this ratio was lowest at the peak of the
459 bloom (2.5 %) when primary production (particulate and dissolved) was highest. These

460 estimates are lower than the bacterial carbon demands of 16 to 36 % of primary production
461 previously determined in the western north Atlantic during spring (Li et al. 1993). The low
462 ratio in the Celtic Sea indicates that a large proportion (i.e. >83 %) of the phytoplankton-
463 produced organic carbon was available for export to depth or for consumption by micro- and
464 meso-zooplankton.

465 Changes in BP, and not in $INT_{0.2-0.8}$, influenced the changes in the BGEs observed during
466 spring, which ranged from <31 % at the beginning of April when BP was low to 40-60 % on
467 20th and 25th April when BP rates were highest. These results are in agreement with the high
468 variability in BGE observed in natural waters (Del Giorgio and Cole 1998; Robinson 2008;
469 Sintes et al. 2010; Guillemette et al. 2016) and can only be explained by an uncoupling of
470 bacterial production and respiration or a shift in the bacterial community structure to
471 predominantly cells with high growth efficiencies (Del Giorgio and Gasol 2008) at the end of
472 the sampling period. The uncoupling could occur through a shift in the bacterial activity from
473 using carbon resources for cell maintenance at the beginning of April to biomass production
474 at the end of April. A recent study of bacterial metabolism in Canadian freshwater lakes
475 showed how bacteria preferred dissolved organic carbon (DOC) from algal sources over that
476 from terrestrial sources (Guillemette et al. 2016). In addition, this study demonstrated how
477 bacteria allocated the DOC to either biomass production or respiration depending on its
478 origin, with more algal DOC being channelled to respiration. Our measurements do not allow
479 us to determine the allocation of organic carbon to bacterial biomass or respiration, but the
480 increase in primary production, phytoplankton-produced dissolved organic carbon and the
481 subsequent increase in bacterial production but not bacterial respiration does indicate
482 different pathways for the carbon.

483 Importantly, our results suggest that calculations of marine carbon budgets should take into
484 account the high variability in BGE observed. This is in direct contrast to previous

485 assumptions of a constant BGE (for example, of 50 % in the Celtic Sea study of Joint et al.
486 2001). Our average BGE of 39 ± 3 % was higher than the average of 20 % reported for many
487 marine systems (Del Giorgio and Cole 1998) but is within the range of BGEs measured in the
488 North Sea during spring (16 – 39 %, Reinthaler and Herndl 2005 and 18 – 43 %, Sintes et al.
489 2010) and in temperate upwelling-induced phytoplankton blooms (34 ± 5 – 52 ± 7 % Teira et
490 al. 2015 and 17 - 62 %, Wear et al. 2015). In common with all other direct determinations of
491 BGE, the BGEs presented here include the bias that while estimates of BP include the
492 production of particle attached bacteria, estimates of the respiration of a bacterial size fraction
493 of the plankton do not.

494 BGEs are affected by temperature (Rivkin and Legendre 2001), inorganic nutrient availability
495 (Rivkin and Anderson 1997; Lønborg et al. 2011) and the quality of the available dissolved
496 organic matter (Goldman et al. 1987; Lemée et al. 2002; Reinthaler and Herndl 2005). We
497 observed a positive correlation between BGE and temperature despite the small range in
498 temperature (9.9 °C – 11.1 °C) which occurred during our study. The inverse covariation
499 between nitrate+nitrite and PP, and the positive correlation between BGE and PP contributed
500 to the negative correlation between BGE and inorganic nitrate+nitrite ($r = -0.77$, $p < 0.0001$, n
501 = 33), contrary to the analysis by Lønborg et al. (2011). The increase in BGE and in BP may
502 have been driven by a change in the quality of the available dissolved organic material
503 (Benner et al. 1995, Jiao et al. 2014), as the DOC:DON ratio decreased slightly from 25 ± 4
504 on the 4th April to 17 ± 3 on the 25th April (Davis et al. this issue). Unfortunately, there are
505 only three days when both DOM composition and bacterial metabolism were measured,
506 precluding any statistical analysis.

507

508 In summary, the strong covariation in the rates of primary production and plankton
509 community respiration during the spring bloom implies that the same physicochemical
510 conditions that stimulated PP also enhanced CR_{O2}. There was no 4-5 day time lag between PP
511 and CR_{O2} in contrast to previous studies of diatom-dominated blooms. The increase in CR_{O2}
512 was driven by an increase in respiration of the >0.8 μm size fraction (presumably
513 phytoplankton and heterotrophic eukaryotes) rather than in free-living bacterial respiration
514 (0.2-0.8 μm size fraction). There was an increase in bacterial production while bacterial
515 respiration was fairly constant throughout the phytoplankton bloom. Changes in bacterial
516 growth efficiencies were driven by changes in bacterial production with values increasing
517 from <31 % at the start of the phytoplankton bloom to 40-60 % at the end of the bloom,
518 suggesting that carbon budgets which rely on a constant BGE could be biased.

519

520 **5. Acknowledgements**

521 We thank the captain and crew of the *RRS Discovery* during DY029 cruise for their help and
522 support at sea and all the scientists involved in the cruise. We would also like to thank Joanne
523 Hopkins and Charlotte Williams (National Oceanographic Centre, Liverpool) for assistance
524 and provision of the physical characterization of the area, E. Malcolm S. Woodward for the
525 nutrient data and Clare E. Davis and Claire Mahaffey for the elemental characterization of the
526 dissolved and particulate organic matter. This study is a contribution to the UK Natural
527 Environment Research Council (NERC) Shelf Sea Biogeochemistry programme. E.EG-M
528 was funded by NERC grant NE/K00168X/1 (awarded to C. Robinson and D. Purdie). SM,
529 EM & CW were funded by NERC grant NE/K001884/1 (awarded to K. Davidson). We thank
530 Ray Leakey for advice with bacterial production methodology and data. GT was funded by

531 NERC grant NE/K002058/1. KM, AJP and CJD were funded by NERC grant NE/K001701/1
532 (awarded to A. Poulton).

533

534 **References**

535 Amon, R. M. W., Benner, R. 1994. Rapid cycling of high-molecular-weight dissolved
536 organic matter in the ocean. *Nature* 369: 549-552.

537 Amon, R. M. W., Benner, R. 1996. Bacterial utilization of different size classes of dissolved
538 organic matter. *Limnology and Oceanography* 41: 41-51.

539 Aranguren-Gassis, M., Teira, E., Serret, P., Martínez-García, S., Fernández, E. 2012.
540 Potential overestimation of bacterial respiration rates in oligotrophic plankton
541 communities. *Marine Ecology Progress Series* 453: 1-10.

542 Azam, F. 1998. Microbial control of oceanic carbon flux: the plot thickens. *Science* 280: 694-
543 696.

544 Barnes, M. K., Tilstone, G. H., Suggett, D. J., Widdicombe, C. E., Bruun, J., Martinez-
545 Vicente, V., Smyth, T. J. 2015. Temporal variability in total, micro-and nano-
546 phytoplankton primary production at a coastal site in the western English Channel.
547 *Progress in Oceanography* 137: 470-483.

548 Behrenfeld, M. J. 2010. Abandoning Sverdrup's critical depth hypothesis on phytoplankton
549 blooms. *Ecology* 91: 977-989.

550 Benner, R., Opshal, S., Chin-Leo, G. 1995. Bacterial carbon metabolism in the Amazon River
551 system. *Limnology and Oceanography* 40(7): 1262-1270.

552 Berggren, M., Lapierre, J.-F., Del Giorgio, P. A. 2012. Magnitude and regulation of
553 bacterioplankton respiratory quotient across freshwater environmental gradients. *The*
554 *ISME journal* 6: 984-993.

555 Biddanda, B., Benner, R. 1997. Carbon, nitrogen, and carbohydrate fluxes during the
556 production of particulate and dissolved organic matter by marine phytoplankton.
557 *Limnology and Oceanography* 42: 506-518.

558 Blight, S., Bentley, T., Lefevre, D., Robinson, C., Rodrigues, R., Rowlands, J., Williams, P.J.
559 le B. 1995. Phasing of autotrophic and heterotrophic plankton metabolism in a temperate
560 coastal ecosystem. *Marine Ecology Progress Series* 128: 61-75.

561 Buchanan, B. B., Gruissem, W., Jones, R. L. 2000. *Biochemistry and molecular biology of*
562 *plants*. American Society of Plant Physiologists Rockville, MD.

563 Caffrey, J. M., Cloern, J. E., Grenz, C. 1998. Changes in production and respiration during a
564 spring phytoplankton bloom in San Francisco Bay, California, USA: implications for net
565 ecosystem metabolism. *Marine Ecology Progress Series* 172: 1-12.

566 Carritt, D. E., Carpenter, J. H. 1966. Comparison and evaluation of currently employed
567 modifications of the Winkler method for determining dissolved oxygen in seawater; a
568 NASCO Report. *Journal of Marine Research* 24: 286-319.

569 D'Alelio, D., Libralato, S., Wyatt, T., D'Alcalà, M. R. 2016. Ecological-network models link
570 diversity, structure and function in the plankton food-web. *Scientific reports* 6:21806 |
571 DOI: 10.1038/srep21806

572 Danger, M., Oumarou, C., Benest, D., Lacroix, G. 2007. Bacteria can control stoichiometry
573 and nutrient limitation of phytoplankton. *Functional Ecology* 21: 202-210

574 Daniels, C. J., Poulton, A. J., Esposito, M., Paulsen, M. L., Bellerby, R., St. John, M., Martin,
575 A. P. 2015. Phytoplankton dynamics in contrasting early stage North Atlantic spring
576 blooms: composition, succession, and potential drivers. *Biogeosciences*, 12, 2395–2409

577 Davis, C. E., Blackbird, S., Wolf, G., Sharples, J., Woodward, E. M. S., Mahaffey, C. This
578 issue. Seasonal organic matter dynamics in a temperate shelf sea. *Progress in*
579 *Oceanography*.

580 Del Giorgio, P. A., Cole, J. J. 1998. Bacterial growth efficiency in natural aquatic systems.
581 *Annual Review of Ecology and Systematics*: 503-541.

582 Del Giorgio, P. A., Gasol, J. M. 2008. Physiological structure and single-cell activity in
583 marine bacterioplankton, p. 243-298. In D. L. Kirchman [ed.], *Microbial Ecology of the*
584 *Oceans*. John Wiley & Sons, Inc.

585 Ducklow, H., Kirchman, D., Quinby, H., Carlson, C., Dam, H. 1993. Stocks and dynamics of
586 bacterioplankton carbon during the spring bloom in the eastern North Atlantic Ocean.
587 *Deep Sea Research Part II: Topical Studies in Oceanography* 40: 245-263.

588 Falkowski, P. G., Owens, T. G. 1980. Light—shade adaptation two strategies in marine
589 phytoplankton. *Plant Physiology* 66: 592-595.

590 Falkowski, P. G., Raven, J. A. 2007. *Aquatic photosynthesis*. 2nd Ed. Princeton University
591 Press.

592 Fasham, M., Holligan, P., Pugh, P. 1983. The spatial and temporal development of the spring
593 phytoplankton bloom in the Celtic Sea, April 1979. *Progress in Oceanography* 12: 87-
594 145.

595 Fernández, E., Serret, P., De Madariaga, I., Harbour, D., Davies, A. 1992. Photosynthetic
596 carbon metabolism and biochemical composition of spring phytoplankton assemblages

597 enclosed in microcosms: the diatom-*Phaeocystis* sp. succession. *Marine Ecology*
598 *Progress Series* 90: 89-102.

599 Fileman, E. S., Fitzgeorge-Balfour, T., Tarran, G. A., Harris, R. P. 2011. Plankton
600 community diversity from bacteria to copepods in bloom and non-bloom conditions in
601 the Celtic Sea in spring. *Estuarine, Coastal and Shelf Science* 93: 403-414.

602 García-Martín, E. E., Aranguren-Gassis, M., Hartmann, M., Zubkov, M. V., Serret, P. 2016.
603 Contribution of bacterial respiration to plankton respiration from 50°N to 44°S in the
604 Atlantic Ocean. *Progress in Oceanography*. doi.org/10.1016/j.pocean.2016.11.006

605 García-Martín E. E., Daniels C. J., Davidson K., Davis C. E., Mahaffey C., Mayers K. M.J.,
606 McNeill S., Poulton A. J., Purdie D. A., Tarran G., Robinson C. Seasonal changes in
607 microplankton respiration and bacterial metabolism in a temperate Shelf Sea. *Progress in*
608 *Oceanography* (this issue), *In rev.*

609 Goldman, J. C., Caron, D. A., Dennett, M. R. 1987. Regulation of gross growth efficiency
610 and ammonium regeneration in bacteria by substrate C: N ratio. *Limnology and*
611 *Oceanography* 32: 1239-1252.

612 Grossart, H.-P., Czub, G., Simon, M. 2006. Algae–bacteria interactions and their effects on
613 aggregation and organic matter flux in the sea. *Environmental Microbiology* 8: 1074-
614 1084.

615 Guillemette, F., Leigh McCallister, S., Del Giorgio, P. A. 2016. Selective consumption and
616 metabolic allocation of terrestrial and algal carbon determine allochthony in lake
617 bacteria. *The ISME Journal* 10: 1373-1382.

618 Henson, S. A., Robinson, I., Allen, J. T., Waniek, J. J. 2006. Effect of meteorological
619 conditions on interannual variability in timing and magnitude of the spring bloom in the

620 Irminger Basin, North Atlantic. Deep Sea Research Part I: Oceanographic Research
621 Papers 53: 1601-1615.

622 Hickman A., Poulton, A.J., Mayers, K. M. J., Tarran, G. A. This issue. Seasonal variability in
623 size-fractionated chlorophyll-a and primary production in the Celtic Sea. Progress in
624 Oceanography.

625 Humphreys M. P., Moore, C. M., Achterberg E. P., Hartman S. E., Kivimäe, C., Griffiths, A.
626 M., Smilenova, A., Chowdhury, M. Z. H., Hull, T., Woodward, E.M.S., Wihsgott, J.,
627 Hopkins, J. E. This issue. Mechanisms for a nutrient-conservative carbon pump in a
628 seasonally stratified, temperate continental shelf sea. Progress in Oceanography.

629 Hydes, D., Aoyama, M., Aminot, A., Bakker, K., Becker, S., Coverly, S., Daniel, A.,
630 Dickson, A., Grosso, O., Kerouel, R. 2010. Recommendations for the determination of
631 nutrients in seawater to high levels of precision and inter-comparability using continuous
632 flow analysers. GO-SHIP (Unesco/IOC).

633 Jiao, N., Robinson, C., Azam, F., Thomas, H., Baltar, F., Dang, H., Hardman-Mountford, N.,
634 Johnson, M., Kirchman, D., Koch, B. 2014. Mechanisms of microbial carbon
635 sequestration in the ocean—future research directions. Biogeosciences 11: 5285-5306.

636 Joint, I., Owens, N., Pomroy, A. 1986. Seasonal production of photosynthetic picoplankton
637 and nanoplankton in the Celtic Sea. Marine Ecology Progress Series 28: 251-258.

638 Joint, I., Wollast, R., Chou, L., Batten, S., Elskens, M., Edwards, E., Hirst, A., Burkill, P.,
639 Groom, S., Gibb, S. 2001. Pelagic production at the Celtic Sea shelf break. Deep Sea
640 Research Part II: Topical Studies in Oceanography 48: 3049-3081.

641 Kirchman, D. 2001. Measuring bacterial biomass production and growth rates from leucine
642 incorporation in natural aquatic environments, p. 227-237. Methods in Microbiology.
643 Academic Press.

644 Lancelot, C. 1984. Extracellular release of small and large molecules by phytoplankton in the
645 southern bight of the North Sea. *Estuarine, coastal and shelf science* 18: 65-77.

646 Landa, M., Blain, S., Christaki, U., Monchy, S., Obernosterer, I. 2015. Shifts in bacterial
647 community composition associated with increased carbon cycling in a mosaic of
648 phytoplankton blooms. *The ISME journal* 10: 39-50.

649 Legendre, L., Le Fèvre, J. 1995. Microbial food webs and the export of biogenic carbon in
650 oceans. *Aquatic Microbial Ecology* 9: 69-77.

651 Lemée, R., Rochelle-Newall, E., Van Wambeke, F., Pizay, M., Rinaldi, P., Gattuso, J. 2002.
652 Seasonal variation of bacterial production, respiration and growth efficiency in the open
653 NW Mediterranean Sea. *Aquatic Microbial Ecology* 29: 227-237.

654 Li, W., Dickie, P., Harrison, W., Irwin, B. 1993. Biomass and production of bacteria and
655 phytoplankton during the spring bloom in the western North Atlantic Ocean. *Deep Sea*
656 *Research Part II: Topical Studies in Oceanography* 40: 307-327.

657 Lønborg, C., Martínez-García, S., Teira, E., Álvarez-Salgado, X. A. 2011. Bacterial carbon
658 demand and growth efficiency in a coastal upwelling system. *Aquatic Microbial Ecology*
659 63: 183-191.

660 Lønborg, C., Nieto-Cid, M., Hernando-Morales, V., Hernández-Ruiz, M., Teira, E., Álvarez-
661 Salgado, X. A. 2016. Photochemical alteration of dissolved organic matter and the
662 subsequent effects on bacterial carbon cycling and diversity. *FEMS microbiology*
663 *ecology* 92: fiw048.

664 López-Sandoval, D., Fernández, A., Marañón, E. 2011. Dissolved and particulate primary
665 production along a longitudinal gradient in the Mediterranean Sea. *Biogeosciences* 8:
666 815-825.

667 Maldonado, F., Packard, T., Gómez, M. 2012. Understanding tetrazolium reduction and the
668 importance of substrates in measuring respiratory electron transport activity. *Journal of*
669 *Experimental Marine Biology and Ecology* 434: 110-118.

670 Marra, J. 2002. Approaches to the measurement of plankton production. In: Williams, P.J. le
671 B., Thomas, D.N., Reynolds, C.S. (Eds), *Phytoplankton Productivity - Carbon*
672 *Assimilation in Marine and Freshwater Ecosystems*. Blackwell Science, pp. 78-108.

673 Martínez-García, S., Fernández, E., Aranguren-Gassis, M., Teira, E. 2009. In vivo electron
674 transport system activity: a method to estimate respiration in natural marine microbial
675 planktonic communities. *Limnology and Oceanography: methods* 7: 459-469.

676 Mayers, K.M.J., Poulton, A.J., Daniels, C.J., Wells, S.R., Woodward, E.M.S., Tyrrell, T.,
677 Giering, S.L.C. This issue. Top-down control of coccolithophore populations during
678 spring in a temperate Shelf Sea (Celtic Sea, April 2015). *Progress in Oceanography*.

679 Miller, J. C., Miller, J. N. 1988. *Statistics for analytical chemistry*. 2nd Ed, Ellis Horwood,
680 Chichester.

681 Moore, C. M., Suggett, D. J., Hickman, A. E., Kim, Y.-N., Tweddle, J. F., Sharples, J.,
682 Geider, R. J., Holligan, P. M. 2006. Phytoplankton photoacclimation and
683 photoadaptation in response to environmental gradients in a shelf sea. *Limnology and*
684 *Oceanography* 51: 936-949.

685 Pedler, B. E., Aluwihare, L. I., Azam, F. 2014. Single bacterial strain capable of significant
686 contribution to carbon cycling in the surface ocean. *Proceedings of the National*
687 *Academy of Sciences* 111: 7202-7207.

688 Pingree, R., Holligan, P., Mardell, G., Head, R. 1976. The influence of physical stability on
689 spring, summer and autumn phytoplankton blooms in the Celtic Sea. *Journal of the*
690 *Marine Biological Association of the United Kingdom* 56: 845-873.

691 Poulton, A. J., Daniels, C. J., Esposito, M., Humphreys, M. P., Mitchell, E., Ribas-Ribas, M.,
692 Russell, B. C., Stinchcombe, M. C., Tynan, E., Richier, S. 2016. Production of dissolved
693 organic carbon by Arctic plankton communities: Responses to elevated carbon dioxide
694 and the availability of light and nutrients. *Deep Sea Research Part II: Topical Studies in*
695 *Oceanography* 127: 60-74.

696 Poulton, A.J., Davis, C.E., Daniels, C.J., Mayers, K.M.J., Harris, C., Tarran, G.A.,
697 Widdicombe, C.E., Woodward, E.M.S. This issue. Seasonal phosphorus dynamics in a
698 temperate shelf sea (Celtic Sea): uptake, release, turnover and stoichiometry. *Progress in*
699 *Oceanography*.

700 Rees, A. P., Joint, I., Donald, K. M. 1999. Early spring bloom phytoplankton-nutrient
701 dynamics at the Celtic Sea Shelf Edge. *Deep Sea Research Part I: Oceanographic*
702 *Research Papers* 46: 483-510.

703 Reinthaler, T., Herndl, G. J. 2005. Seasonal dynamics of bacterial growth efficiencies in
704 relation to phytoplankton in the southern North Sea. *Aquatic Microbial Ecology* 39: 7-
705 16.

706 Rivkin, R. B., Anderson, M. R. 1997. Inorganic nutrient limitation of oceanic
707 bacterioplankton. *Limnology and Oceanography* 42: 730-740.

708 Rivkin, R. B., Legendre, L. 2001. Biogenic carbon cycling in the upper ocean: effects of
709 microbial respiration. *Science* 291: 2398-2400.

710 Robinson, C. 2008. Heterotrophic Bacterial Respiration, p. 299-334. In D. L. Kirchman [ed.],
711 *Microbial Ecology of the Oceans*. John Wiley & Sons, Inc.

712 Robinson, C., Williams, P.J. le B. 1999. Plankton net community production and dark
713 respiration in the Arabian Sea during September 1994. *Deep Sea Research Part II:*
714 *Topical Studies in Oceanography* 46: 745-765.

715 Schlitzer, R. 2015. Ocean Data View, <http://odv.awi.de>

716 Sherr, E., Sherr, B. 1994. Bacterivory and herbivory: key roles of phagotrophic protists in
717 pelagic food webs. *Microbial Ecology* 28: 223-235.

718 Sintes, E., Stoderegger, K., Parada, V., Herndl, G. J. 2010. Seasonal dynamics of dissolved
719 organic matter and microbial activity in the coastal North Sea. *Aquatic Microbial*
720 *Ecology* 60: 85.

721 Smith, D. C., Steward, G. F., Long, R. A., Azam, F. 1995. Bacterial mediation of carbon
722 fluxes during a diatom bloom in a mesocosm. *Deep sea research part II: Topical Studies*
723 *in Oceanography* 42: 75-97.

724 Smyth, T. J., Allen, I., Atkinson, A., Bruun, J. T., Harmer, R. A., Pingree, R. D.,
725 Widdicombe, C. E., Somerfield, P. J. 2014. Ocean Net Heat Flux Influences Seasonal to
726 Interannual Patterns of Plankton Abundance. *PLoS ONE* 9: e98709.

727 Stewart, J. C., Hawcroft, D. M. 1977. *A manual of radiobiology*. University of Washington
728 Press, Seattle.

729 Tada, Y., Taniguchi, A., Nagao, I., Miki, T., Uematsu, M., Tsuda, A., Hamasaki, K. 2011.
730 Differing growth responses of major phylogenetic groups of marine bacteria to natural
731 phytoplankton blooms in the western North Pacific Ocean. *Applied and Environmental*
732 *Microbiology* 77: 4055-4065.

733 Tarran, G. A., Heywood, J. L., Zubkov, M. V. 2006. Latitudinal changes in the standing
734 stocks of nano- and picoeukaryotic phytoplankton in the Atlantic Ocean. *Deep Sea*
735 *Research Part II: Topical Studies in Oceanography* 53: 1516-1529.

736 Taylor, A. H., Geider, R. J., Gilbert, F. J. 1997. Seasonal and latitudinal dependencies of
737 phytoplankton carbon-to-Chl a ratios: results of a modelling study. *Marine Ecology*
738 *Progress Series* 152: 51-66.

739 Teira, E., Hernando-Morales, V., Fernández, A., Martínez-García, S., Álvarez-Salgado, X.,
740 Bode, A., Varela, M. 2015. Local differences in phytoplankton– bacterioplankton
741 coupling in the coastal upwelling off Galicia (NW Spain). *Marine Ecology Progress*
742 *Series 528*: 53-69.

743 Van Oostende, N., Harlay, J., Vanelslander, B., Chou, L., Vyverman, W., Sabbe, K. 2012.
744 Phytoplankton community dynamics during late spring coccolithophore blooms at the
745 continental margin of the Celtic Sea (North East Atlantic, 2006–2008). *Progress in*
746 *Oceanography 104*: 1-16.

747 Wear, E. K., Carlson, C. A., James, A. K., Brzezinski, M. A., Windecker, L. A., Nelson, C. E.
748 2015. Synchronous shifts in dissolved organic carbon bioavailability and bacterial
749 community responses over the course of an upwelling-driven phytoplankton bloom.
750 *Limnology and Oceanography 60*: 657-677.

751 Widdicombe, C., Eloire, D., Harbour, D., Harris, R., Somerfield, P. 2010. Long-term
752 phytoplankton community dynamics in the Western English Channel. *Journal of*
753 *Plankton Research 32*: 643-655.

754 Wihsgott J. U., Sharples J., Hopkins J. E., Woodward E. M. S., Greenwood N., Hull T.,
755 Sivyer D. B. This issue. Investigating the autumn bloom's significance within the
756 seasonal cycle of primary production in a temperate shelf sea. *Progress in Oceanography*.
757 *In rev.*

758 Williams, P.J. le B., del Giorgio, P. A. 2005. Respiration in aquatic ecosystems: history and
759 background, p. 1-17. In P. A. del Giorgio and P.J. le B. Williams [eds.], *Respiration in*
760 *aquatic ecosystems*. Oxford University Press.

761 Woodward, E.M.S., and Rees, A. 2001. Nutrient distributions in an anticyclonic eddy in the
762 northeast Atlantic Ocean, with reference to nanomolar ammonium concentrations. *Deep*
763 *Sea Research Part II: Topical Studies in Oceanography* 48: 775-793.

764

765

Table 1. Characterization of the central Celtic Sea (CCS) sampling station: euphotic depth (depth of 1% surface irradiance), depth of the pycnocline, surface temperature, and range of nitrate+nitrite and phosphate concentrations in the euphotic zone.

Sampling day	Depth 1% I ₀ (m)	Depth pycnocline (m)	Temperature (°C)	Nitrate +nitrite (μM)	Phosphate (μM)
04/04/2015	37	51	9.9	6 - 6.1	0.5
06/04/2015	37	47	9.9	5.6 - 5.7	0.4 - 0.5
11/04/2015	32	30	10.3	3.8 - 4.9	0.3 - 0.4
15/04/2015	28	15	10.7	1.3 - 4.1	0.2 - 0.4
20/04/2015	28	30	10.6	2 - 2.9	0.2 - 0.3
25/04/2015	35	16	11.1	0.4 - 2.8	0.1 - 0.2

Table 2. Euphotic depth-integrated chlorophyll-*a* concentrations (Chl-*a*), daily plankton community respiration (CR_{O2}), bacterial respiration (INT_{0.2-0.8}), percentage of bacterial respiration (%INT_{0.2-0.8}), bacterial production (BP), gross primary production (PP) and the balance between primary production and plankton respiration (PP - CR_{O2}) measured during April 2015 (\pm SE, except for PP which is \pm SD). nd denotes no data. Chl-*a* values are presented in Hickman et al. this issue.

Sampling day	Chl- <i>a</i> mg Chl- <i>a</i> m ⁻²	CR _{O2} mmol O ₂ m ⁻² d ⁻¹	INT _{0.2-0.8} mmol O ₂ m ⁻² d ⁻¹	% INT _{0.2-0.8} %	BP mg C m ⁻² d ⁻¹	PP mmol C m ⁻² d ⁻¹	PP - CR _{O2} mmol C m ⁻² d ⁻¹
04/04/2015	49.6	22 \pm 3.6	16.0 \pm 2.9	37.4 \pm 9.8	48.2 \pm 2.7	114.5 \pm 4.6	92.5 \pm 5.8
06/04/2015	61.4	47.5 \pm 4.9	nd	nd	52.7 \pm 1.8	148.2 \pm 7.4	100.7 \pm 8.9
11/04/2015	94.9	77.2 \pm 4	8.2 \pm 1.5	13.2 \pm 2.6	112.1 \pm 4.3	314.3 \pm 16	237.1 \pm 23.3
15/04/2015	152.6	119.2 \pm 3.6	13.7 \pm 1.9	15.9 \pm 2.4	118.2 \pm 4.7	613 \pm 27.7	493.8 \pm 27.9
20/04/2015	96.6	84.8 \pm 3.3	10.4 \pm 1.3	12.3 \pm 1.6	132.7 \pm 7.3	264.2 \pm 38.2	179.4 \pm 33.1
25/04/2015	109.2	147 \pm 4.2	10.8 \pm 0.6	16.3 \pm 1.2	128.7 \pm 3.0	304.1 \pm 9.9	157.1 \pm 10.7

LEGEND

Figure 1. Location of the Central Celtic Sea sampling station in the Celtic Sea.

Figure 2. Potential density during April 2015 at the CCS station. Smaller black dots represent the CTD data used to derive the contour plot ($n = 40$ vertical profiles), larger black dots show the depths where water samples were collected and the white dotted line is the euphotic depth (1 % surface irradiance).

Figure 3. Vertical profiles of (A) chlorophyll-*a* concentration ($\mu\text{g Chl-}a \text{ L}^{-1}$), (B) primary production ($\mu\text{mol C L}^{-1} \text{ d}^{-1}$) and (C) bacterial abundance ($10^6 \text{ cells mL}^{-1}$) during April 2015.

Figure 4. Vertical profiles of (A) plankton community respiration (INT_T), (B) plankton community respiration (CR_{O_2}), (C) respiration of the plankton fraction $>0.8 \mu\text{m}$ ($\text{INT}_{>0.8}$), (D) bacterial respiration ($\text{INT}_{0.2-0.8}$), (E) bacterial production (BP) and (F) bacterial growth efficiency (BGE) during April 2015. Error bars represent the standard error between sample bottles.

Figure 5. Vertical profiles of cell-specific bacterial respiration (A) and bacterial production (B) during April 2015. Error bars represent the standard error of the measurements.

Figure 6. Relationship between the bacterial carbon demand (BCD) and the locally produced organic carbon available for the bacteria, considered as the sum of particulate organic carbon (PP) and dissolved organic carbon production ($p\text{DOC}$) minus the respiration of the autotrophic plankton ($\text{INT}_{>0.8}$). Lines represent when the BCD: ($\text{PP} + p\text{DOC} - \text{INT}_{>0.8}$) ratio equals 5 (solid line) and 10 % (dashed line).

Figure 7. Relationship between: (A) bacterial respiration ($\text{INT}_{0.2-0.8}$) and (B) bacterial production (BP) and bacterial growth efficiency (BGE) throughout the water column. Error bars represent the standard error of the measurements and the solid lines the corresponding

linear regression with R^2 the coefficient of determination, p the level of significance and n the number of data.

Figure 1.

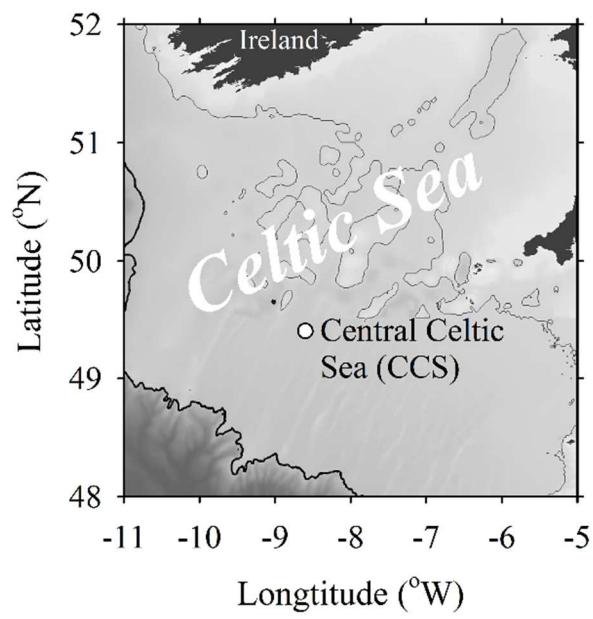


Figure 2.

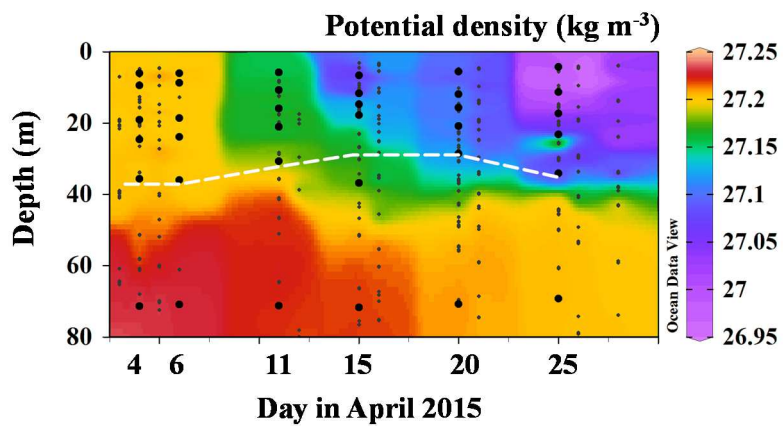


Figure 3.

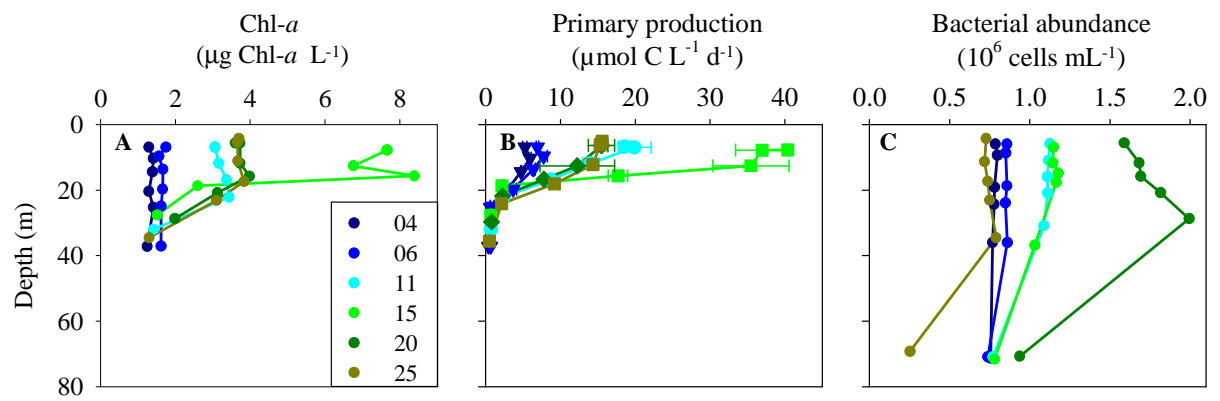


Figure 4.

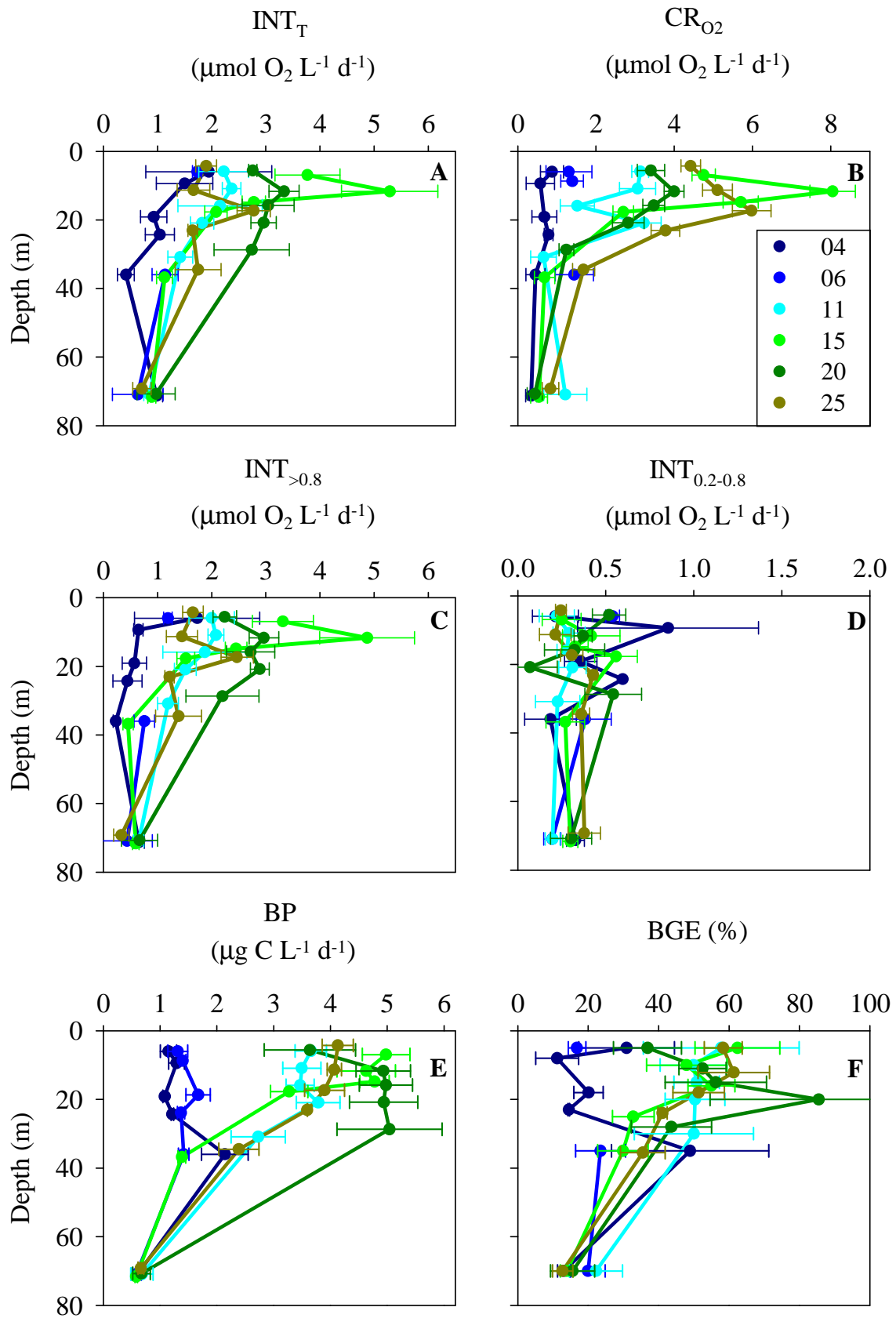


Figure 5.

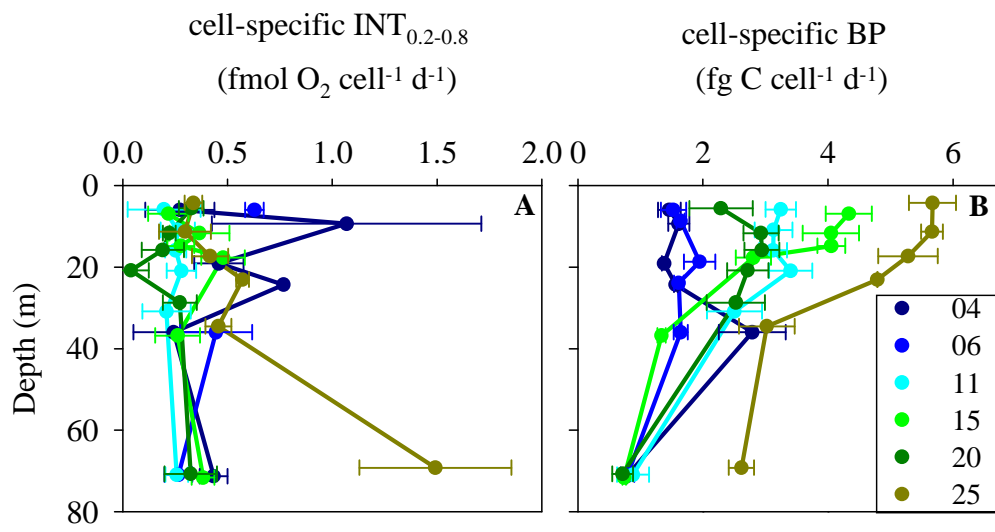


Figure 6.

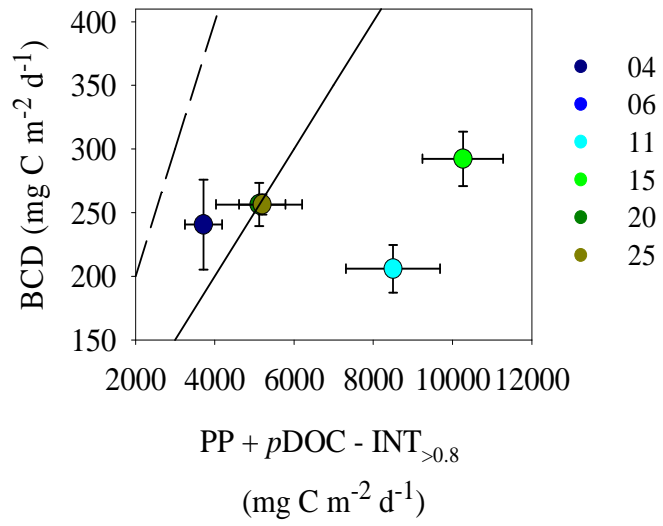


Figure 7.

